Radiance in a Dynamic Ocean (RaDyO): Radiance and Visibility as Affected by Inherent Optical Properties

Grace Chang
Sea Engineering, Inc.
200 Washington St., Suite 210
Santa Cruz, CA 95060
phone: (831) 421-0871 fax: (831) 421-0875 email: gchang@seaengineering.com

Award Number: N0001409C0443

LONG-TERM GOALS

The long-term goal of "Radiance in a Dynamic Ocean (RaDyO): Radiance and Visibility as Affected by Inherent Optical Properties" is to perform detailed investigations of inherent optical properties (IOPs) and the effects of IOP variability on underwater radiance and visibility. As part of this effort, Sea Engineering, Inc. (SEI) will also provide all data from the Scripps Pier and Santa Barbara Channel (SBC) RaDyO experiments to the ONR and to all other RaDyO investigators, with a detailed report describing the technical approach and algorithms used for data processing.

OBJECTIVES

The primary objectives of the Radiance in a Dynamic Ocean (RaDyO) program are to:

1) Examine time-dependent oceanic radiance distribution in relation to dynamic surface boundary layer (SBL) processes.
2) Construct a radiance-based SBL model.
3) Validate the model with field observations.
4) Investigate the feasibility of inverting the model to yield SBL conditions.

As part of the RaDyO project, SEI has performed RaDyO IOP data processing and analysis including data sharing with other RaDyO PIs. Data post-processing includes application of field-calibrations, corrections for temperature, salinity, and scattering effects, and comparisons with similar IOP data collected by RaDyO collaborators.

IOP data analysis as related to the RaDyO program includes detailed investigations of the differences between optical properties and optical variability measured off the R/P FLIP and off the R/V Kilo Moana (KM) during the RaDyO SBC experiment and the effects of optical variability on the modeling of the underwater radiance distribution and visibility.

Efforts to quantify relationships between physical processes and image performance parameters (point spread function, PSF, and modulation transfer function, MTF) and visibility have just begun. The aim

Report Documentation Page

Form Approved
OMB No. 0704-0188

1. REPORT DATE	2. REPORT TYPE	3. DATES COVERED
2010		**00-00-2010 to 00-00-2010**

4. TITLE AND SUBTITLE	5a. CONTRACT NUMBER
Radiance in a Dynamic Ocean (RaDyO): Radiance and Visibility as Affected by Inherent Optical Properties	5b. GRANT NUMBER
	5c. PROGRAM ELEMENT NUMBER
6. AUTHOR(S)	5d. PROJECT NUMBER
	5e. TASK NUMBER
	5f. WORK UNIT NUMBER
7. PERFORMING ORGANIZATION NAME(S) AND ADDRESS(ES) **Sea Engineering, Inc,200 Washington St., Suite 210,Santa Cruz,CA,95060**	8. PERFORMING ORGANIZATION REPORT NUMBER
9. SPONSORING/MONITORING AGENCY NAME(S) AND ADDRESS(ES)	10. SPONSOR/MONITOR'S ACRONYM(S)
	11. SPONSOR/MONITOR'S REPORT NUMBER(S)

12. DISTRIBUTION/AVAILABILITY STATEMENT
Approved for public release; distribution unlimited

13. SUPPLEMENTARY NOTES

14. ABSTRACT

15. SUBJECT TERMS

16. SECURITY CLASSIFICATION OF:			17. LIMITATION OF ABSTRACT	18. NUMBER OF PAGES	19a. NAME OF RESPONSIBLE PERSON
a. REPORT	b. ABSTRACT	c. THIS PAGE			
unclassified	**unclassified**	**unclassified**	**Same as Report (SAR)**	**11**	

of this work is to determine the feasibility of enhancing or restoring images modulated by underwater scattering effects.

APPROACH

The measurement approach for the Scripps Pier and SBC experiments involved the use of a ship-based optical profiler package with the following sensors: SeaBird Electronics, Inc. conductivity-temperature-depth (CTD) (SBE49), WET Labs, Inc. ac-s (86- or 87-wavelengths), ac-9 (with 0.2 μm filter), bb-9, ECOFL-NTU, and Sequoia Scientific, Inc. LISST-100X Type C (Figure 1).

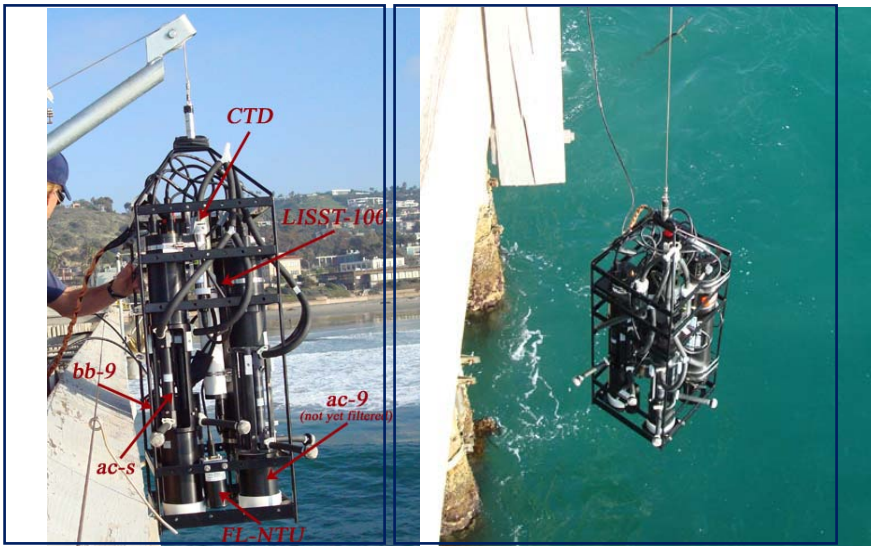

Figure 1. Photographs of the optical profiling package in operation at Scripps Pier in January 2008. Individual sensors are labeled in the photograph on the left.

Data collection during the Scripps Pier experiment was from 14 to 24 January 2008. Our optical profiler was operated on average five times per day between 1000 and 1600 local time (Pacific Standard Time, PST) except one period of night time sampling, performed in conjunction with L. Lenain's (Scripps Institution for Oceanography, SIO) "Cadillac" data collection including light-box images. The depth of data collection ranged between 4 and 7 m, depending on tidal conditions. The participants were: G. Chang, F. Nencioli (University of California, Santa Barbara), F. Spada, and A. Whitmire (Oregon State University).

SBC data were collected from the R/P FLIP between 11 and 20 September 2008. Our optical profiler was operated from the face boom between 11 and 14 September and then from the starboard boom on the 17th and 20th of September (Figure 2). Profile times (1230 and 1600 local time) were coordinated with WET Labs, Inc. MASCOT package sampling periods (from the KM). Face boom casts were taken to 30 m over a 20 minute sampling period. The optical profiler was left in-water between casts and shallow (2 m) time series were collected for 10 minutes every hour between deep casts. Starboard boom sampling consisted of only 30 m casts at time periods when FLIP crew members were available to assist in data collection. These deep casts were also to 30 m, over 45 minute sampling periods.

In addition to the optical profiler, an instrumentation package was mounted on the hull of the FLIP, at 30 m. The sensors on the package included: WET Labs, Inc. ac-s, ECObb-3, and Water Quality Monitor (WQM). The WQM provides time series of temperature, salinity, chlorophyll fluorescence, turbidity, and dissolved oxygen. The sampling rate was once per minute for the WQM and once per hour for the other sensors. The SBC participants were: G. Chang, F. Nencioli, and F. Spada.

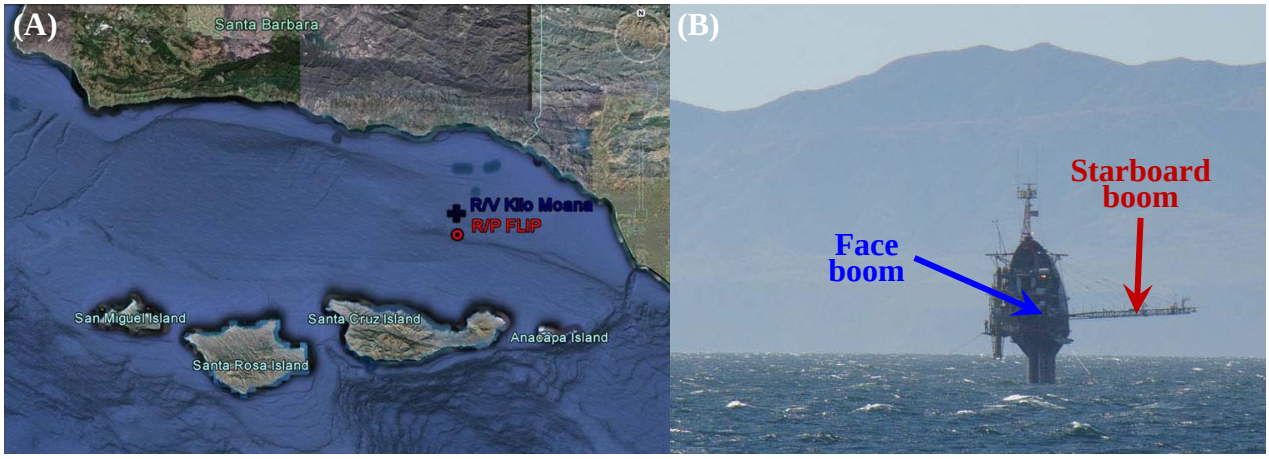

Figure 2. (A) Map of the Santa Barbara Channel, CA with locations of the R/V Kilo Moana (blue cross) and R/P FLIP (red dot) indicated. (B) Photograph of the FLIP taken on 19 September 2008 in the SBC with the face boom and starboard booms indicated. Santa Cruz Island can be seen in background. Photo by Frank Spada.

The data processing and analysis approach utilized factory-recommended and published calibration and correction procedures for IOP sensors (e.g., Zaneveld et al., 1994; Pegau et al., 1997; Sullivan et al., 2006; Zhang et al., 2009) and computations of optical products following methods described by Boss et al. (2001) and Twardowski et al. (2001). Underwater radiance fields were computed from measured IOPs using the radiative transfer model, Hydrolight. Horizontal visibility was estimated from the beam attenuation coefficient using the simplified visibility equation provided by Zaneveld and Pegau (2003). PSFs and MTFs were computed using measured IOPs and empirical or analytical solutions described by Duntley (1971) and Voss (1991), and Hou et al. (2007). Wavelet analysis has been performed on image performance parameters and physical forcing variables in order to determine the dominant scales of variability and coherence, and the periods at which they occur (Grinsted et al., 2004). Data processing and analysis was performed by G. Chang and A. Whitmire (SIO Pier LISST).

WORK COMPLETED

All data collected during the RaDyO SIO Pier and SBC field experiments have been processed, quality assured / quality controlled, and distributed to RaDyO investigators via UCSB's website (http://www.opl.ucsb.edu/ucsbradyo/siopier/siopierdata.html; SIO Pier data) and SEI's FTP site (http://ftp.seaengineering.com/ftp/RaDyO_GCS/; login: SEI_Guest, password: SEI_Guest; SBC data).

Concurrent profiles of optical properties collected from the FLIP and the KM during the SBC experiment were analyzed for optical variability. The effects of optical variability on the underwater

radiance field and visibility have been explored. The paper, "Platform effects on optical variability and the prediction of underwater visibility," by G. Chang, M. S. Twardowski, Y. You, M. Moline, P.-W. Zhai, S. Freeman, M. Slivkoff, F. Nencioli, and G. W. Kattawar was published in Applied Optics in May 2010.

Optical properties collected at 2-m water depth from SIO Pier and in the SBC were used to compute point spread functions, modulation transfer functions, and horizontal visibility. Time series of the image performance parameters and visibility were statistically analyzed with physical forcing parameters (wind speed, wind stress, current velocity, temperature, salinity, and density) and optical properties and products (IOPs, chlorophyll concentration, slope of the spectral particulate beam attenuation coefficient and the real index of refraction of particles; Boss et al., 2001; Twardowski et al., 2001) in order to determine the factors influencing image modulation and visibility. The extended abstract, "Point spread functions and visibility: Gaining clarity on image processing in natural waters," has been submitted to the Ocean Optics Conference for a poster presentation.

RESULTS

A diurnal wind pattern was observed during the two-week SBC experiment. Winds were generally calm (< 4 m/s) in the mornings, and increased to greater than 6 m/s, oftentimes reaching 10 m/s by 1600 PDT. Starting on 15 September, winds greater than about 5 m/s were sustained over the course of two days. The persistent winds resulted in increased upper water column mixing, as evidenced by the increase in 30 m temperature and salinity and the deepening of the mixed layer depth.

We show that the majority of optical variability between the FLIP and the KM was due primarily to platform effects, specifically the break-down of stratification from mixing by the hull of R/P FLIP when winds were less than 5 m/s (Figure 3; Chang et al., 2010). Differing vertical patterns in hydrographic properties and dissimilar vertical distributions of water constituents (and therefore optical properties) observed between the KM and FLIP were the consequence of FLIP-induced mixing. The FLIP-effect was not a factor during higher wind speeds, as the upper water column was well-mixed at both platform locations. Note that the FLIP was moored during the Santa Barbara Channel RaDyO experiment. The FLIP in free-drifting mode, where it is allowed to ride with oceanic motion, may not be as strongly affected by wind-induced mixing.

The observed variable vertical distributions in optical properties greatly affected modeled underwater radiance distribution and predictions of horizontal visibility (Figure 4). Hydrolight-modeled radiometric properties and AOPs differed by about 50% between the KM and FLIP sites during stratified, low wind conditions, as compared to less than 10% during well-mixed periods. The attenuation-based model presented by Zaneveld and Pegau (2003) and a backward Monte-Carlo model were used to predict the horizontal visibility of a black target for high wind and low wind conditions. Results from both models were consistent. Our results show that highly variable IOPs observed between the FLIP and KM during low winds can affect predictions of visibility by up to 57%. Differences were less than 15% between KM and FLIP predicted visibility range during well-mixed periods.

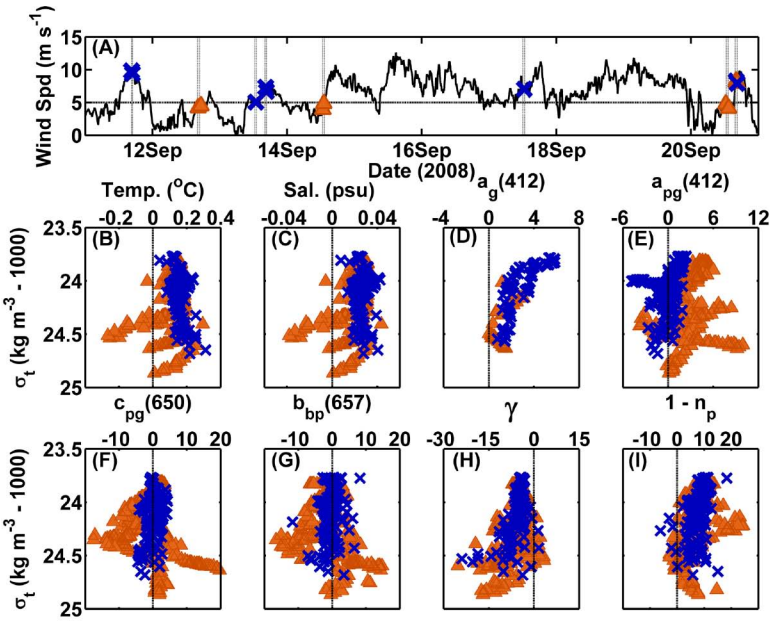

Figure 3. (A) Time series of wind speed collected from the KM. Crosses and triangles indicate periods of KM optical profiler data collection. Light gray, vertical dashed lines denote concurrent KM and FLIP optical profiler data collection. (B-I) Profiles of percent differences between various properties measured from the KM versus from the FLIP as a function of density, σ_t. The units for $a_g(412)$, $a_{pg}(412)$, $c_{pg}(650)$, and $b_{bp}(657)$ are m^{-1}. Crosses indicate periods of data collection with wind speeds ≥ 5 m/s and triangles represent wind speeds < 5 m/s (except the last profile).

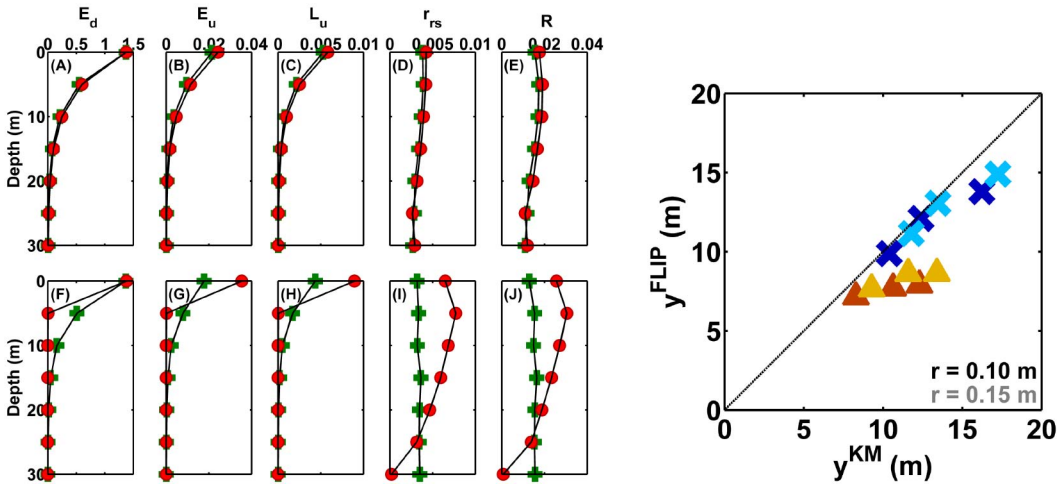

Figure 4. Left: Vertical profiles of radiometric and apparent optical properties modeled using Hydrolight during (A-E) high wind conditions on 13 September 2008 at 1251 PDT and (F-J) low wind conditions on 20 September 2008 at 1225 PDT. Pluses represent KM data and y circles denote FLIP data. Units for E_d and E_u are W m^{-2} nm^{-1}, for Lu are W m^{-2} nm^{-1} sr^{-1}, and for r_{rs} is sr^{-1} (R is dimensionless). Right: Comparisons between computed horizontal visibility of a black target, y, using data collected from the KM versus from the FLIP. Crosses and triangles denote data collected during high wind and low wind conditions, respectively. Dark and light symbols signify results for targets with a diameter of 0.2 and 0.3 m (radius of 0.1 and 0.15 m), respectively.

The strong diurnal signal in winds was also observed in time series of 2-m hydrographic and optical properties and the imaging performance parameters. Hydrographic properties suggest upper water column mixing during the period of sustained high wind speeds (15 – 17 September) and toward the end of the experiment (20 September). The cause of the latter mixing event is unknown. Increases in scattering properties are observed during the two mixing events (15 and 20 September; not shown). Consequently, the imaging performance parameters and visibility followed a similar temporal pattern (180° phase) as the IOPs and the wind speed and wind stress (Figure 5). The slope of the PSF was greatly reduced and visibility decreased during high wind speeds and mixed periods.

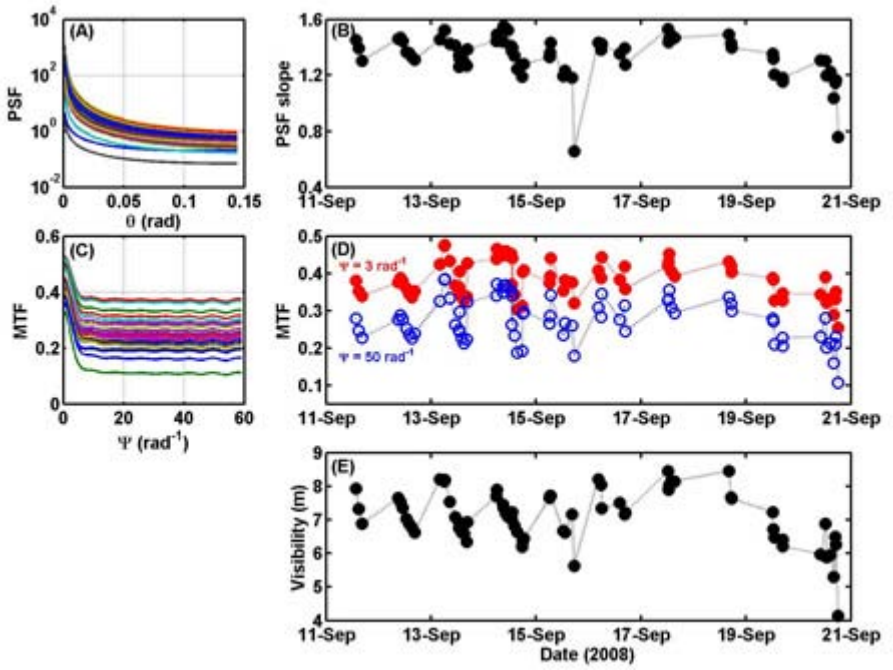

Figure 5. Computed (A) and (C) PSF and MTF; and time series of (B) PSF slope (Voss, 1991), (D) MTF (at 3 rad^{-1} and 50 rad^{-1}), and (E) horizontal visibility of a black target (Zaneveld and Pegau, 2003) from 2-m optical time series collected in the SBC.

Wavelet results indicate that the slope of the PSF and MTF and horizontal visibility are significantly coherent with all featured properties except $b_{bp}(532)$ (nor salinity, not shown) at the diurnal frequency at the beginning of the experiment period (Figure 6). This coherency continues through 17 September for wind speed and stress (not shown), density, $c_{pg}(532)$, $b_p(532)$ (not shown), b_{bp}/b_p (not shown), n_p, and γ and through 14 September for $a_{pg}(532)$ and Chl. Significant coherence is also observed at higher frequencies (0.25 to 0.5 day) for all properties except $b_{bp}(532)$ and salinity between 13 and 15 September and/or 15 and 17 September. Coherence phase arrows indicate that wind speed and stress slightly lead the variability in imaging performance parameters and visibility. PSF, MTF, and visibility are positively related to σ_t and γ and negatively related to $c_{pg}(532)$, $b_p(532)$, and n_p. Visibility is, not surprisingly, strongly negatively coherent with $c_{pg}(532)$ at all time periods and frequencies of data collection (not shown).

The range of values for the imaging performance parameters and visibility were similar between SIO Pier and SBC (Figure 7), which was surprising given the dynamic forcing at the shallow-water SIO Pier site. We expected much better image transmission at the deeper SBC site, however strong winds during the SBC experiment time period appeared to have clouded our hypothesis. Although the scattering coefficients and imaging performance parameters are inversely correlated, the highly scattering minerogenic particles observed at the SIO Pier site did not result in greatly reduced image transmission or visibility when using equations with the β-approximation (e.g., Hou et al., 2007). However, MTF increased significantly during observed rip currents when evaluating the MTF with measured VSFs (Figure 7E and G). Visibility ranged between 4 and 12 m and PSF slope varied between 0.8 and 1.7, similar to the values in the SBC (Figure 7D-G).

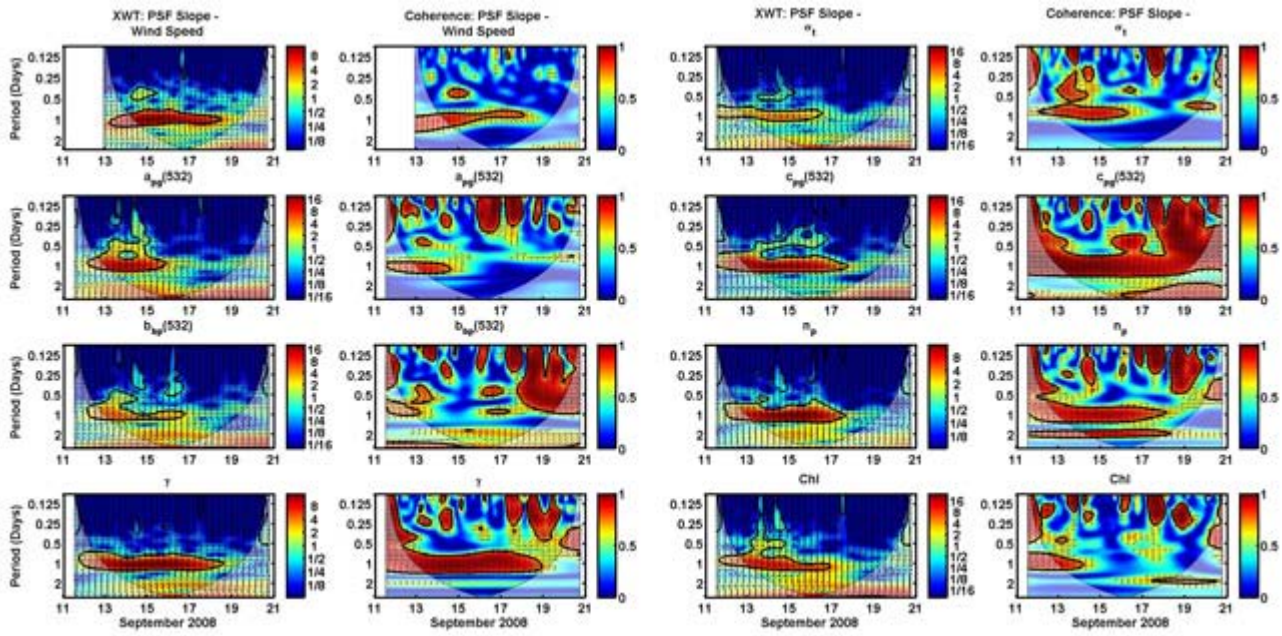

Figure 6. Cross wavelet transforms (XWTs) and wavelet coherence (indicated above each column) computed for various parameters (indicated above each plot) with PSF slope. Frequencies are shown in the y-axis (in days) and the time period of measurements is along the x-axis (date in September 2008). The "cone of influence" (COI) is outlined; regions outside the COI are ignored here. Periods of high wavelet power with statistical significance are shown in deep red and outlined in thick, black lines. In order to determine statistically significant coherency, both the XWT and wavelet coherence figures must be interpreted together (i.e. where both XWT and coherence show strong, common frequency peaks). Arrows indicate the phase direction between the two properties.

Results from this analysis suggest that optical properties, including the imaging performance parameters and visibility were strongly influenced by meteorological processes during the SBC experiment. Increased wind speeds and stresses resulted in upper water column mixing, decreased water clarity, and reductions in image transmission and visibility. Optically-derived particle characteristics such as relative density and particle size distribution (PSD) are also shown to be related to the variability of imaging performance parameters. A decrease in PSD and an increase in relative particle density accompanied reduced image transmission and visibility, likely due to the enhanced effects of multiple scattering for smaller, denser particles.

The optical properties measured at SIO Pier appeared to have been influenced primarily by advective and biological processes. Despite the dynamic and shallow-water environment at SIO Pier, image transmission was found to be similar to that in the SBC. The presence of high concentrations of minerogenic particles observed during rip currents at the Pier resulted in decreased image transmission when using measured near-forward VSFs for computations of the MTF.

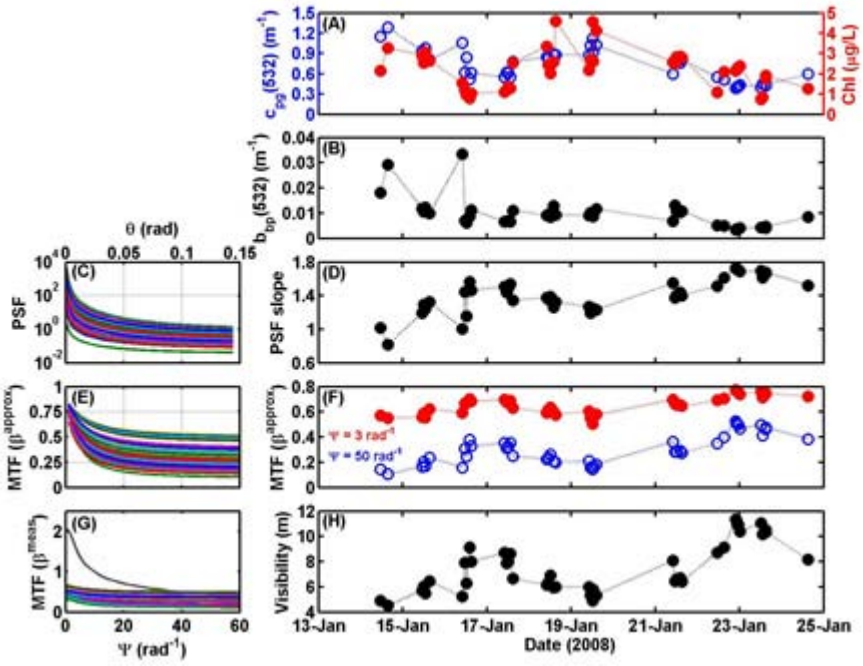

Figure 7. Time series of (A) attenuation at 532 nm and chlorophyll concentration, (B), backscattering at 532 nm; and computed (D) PSF slope, (F) MTF (at 3 and 50 rad^{-1}), and (H) horizontal visibility; (C), PSF, (E) and (G) MTF computed using β-approximation and measured-β, respectively. All data were collected at 2-m at SIO Pier.

IMPACT/APPLICATIONS

Our results have the potential to greatly impact the modeling of underwater radiance distribution for the RaDyO project. The hull of FLIP itself has the capability to mix the upper water column and affect SBL processes. Physical measurements conducted by RaDyO PIs off the FLIP are likely compromised. Additionally, IOPs were not collected off the FLIP during the Hawaii experiment. The FLIP-effect cannot be evaluated for the Hawaii RaDyO field data set. Model(s) will be constructed and/or validated with physical, radiometric, and apparent optical property (AOP) measurements collected off the FLIP and IOP measurements collected off the KM, which was several km away.

The comprehensive optical data set collected as part of the RaDyO program affords the opportunity to make direct computations of imaging modulation parameters using field-measured data, including small-angle VSFs. It also allows the investigation of physical and hydrographic effects on image modulation in two different environments.

RELATED PROJECTS

"Prediction of Optical Variability in Dynamic Nearshore Environments," funded by the National Defense Center of Excellence for Research in Ocean Sciences (CEROS), is a related project (PIs: Chang, Jones, Hansen, Twardowski, and Barnard). The objective of this project is to develop a system for forecasting marine optical conditions in the surf zone for the purpose of improving Naval operations. With our in situ optical forecast model, the Navy Fleet will be able to deploy remote

drifters, combine drifter data with meteorological and oceanographic data within our model, and predict optical properties along a coastline of interest.

Numerical wave and hydrodynamic models have been developed and validated with field measurements obtained by moored platforms and optical floats and drifters in two surf zone environments: Santa Cruz, CA and Waimanalo, HI. A third, validation field experiment will commence in early September 2010 in Duck, NC.

REFERENCES

Agrawal, Y. C. (2005) The optical volume scattering function: Temporal and vertical variability in the water column off the New Jersey coast, Limnol. Oceanogr., 50, 1787-1794.

Boss, E. and W. S. Pegau (2001) Relationships of light scattering at an angle in the backward direction to the backscattering coefficient, Appl. Opt., 40, 5503-5507.

Boss E., M. S. Twardowski, and S. Herring (2001) Shape of the particulate beam attenuation spectrum and its inversion to obtain the shape of the particle size distribution, Appl. Opt., 40, 4885-4893.

Chang, G., M. S. Twardoski, Y. You, M. Moline, P.-W. Zhai, S. Freeman, M. Slivkoff, F. Nencioli, and G. W. Kattawar (2010) Platform effects on optical variability and prediction of underwater visibility, Appl. Opt., 49(15), 2784-2796.

Duntley, S. Q. (1971) Underwater lighting by submerged lasers and incandescent sources, SIO, UC San Diego.

Grinsted, A., J. C Moore, and S. Jevrejeva (2004) Application of the cross wavelet transform and wavelet coherence to geophysical time series, Nonlin. Proc. in Geophys., 11, 561-566.

Hou, W., Z. Lee, and A. D. Weidemann (2007) Why does the Secchi disk disappear? An Imaging perspective, Opt. Expr., 15, 2791-2802.

Pegau, W. S., D. Gray, and J. R. V. Zaneveld (1997) Absorption and attenuation of visible and near-infrared light in water: dependence on temperature and salinity, Appl. Opt., 36, 6035-6046.

Sullivan, J. M., M. S. Twardowski, J. R. V. Zaneveld, C. M. Moore, A. H. Barnard, P. L. Donaghay, and B. Rhoades (2006) Hyperspectral temperature and salt dependencies of absorption by water and heavy water in the 400-750 nm spectral range, Appl. Opt., 45, 5294-5309.

Twardowski, M. S., E. Boss, J. B. Macdonald, W. S. Pegau, A. H. Barnard, and J. R. V. Zaneveld (2001) A model for estimating bulk refractive index from the optical backscattering ratio and the implications for understanding particle composition in case I and case II waters, J. Geophys. Res., 106, 14,129-14,142.

Voss, K. (1991) Simple empirical model of the oceanic point spread function, Appl. Opt., 30, 2647-2651.

Zaneveld, J. R. V. and W. S. Pegau (2003) Robust underwater visibility parameter, Opt. Expr., 11, 2997-3009.

Zaneveld, J. R. V., J. C. Kitchen, and C. M. Moore (1994) Scattering error correction of reflecting-tube absorption meters, in Ocean Optics XII, J. S. Jeffe (Ed.), Proc. SPIE 2258, 44-55.

Zhang, X., L. Hu, and M-X. He (2009) Scattering by pure seawater: Effect of salinity, Opt. Expr., 17, 5698-5710.

PUBLICATIONS

Chang, G., M. S. Twardoski, Y. You, M. Moline, P.-W. Zhai, S. Freeman, M. Slivkoff, F. Nencioli, and G. W. Kattawar (2010) Platform effects on optical variability and prediction of underwater visibility, Appl. Opt., 49(15), 2784-2796.